Photochemical Hydrogen Evolution in $K_4Nb_6O_{17}$ Semiconductor Particles Sensitized by Phosphonated Trisbipyridine Ruthenium Complexes

Young Hee Jung, Hyun Kwan Shim, Hyun Woo Kim, and Yeong Il Kim*

*Department of Chemistry, Pukyong National University, Busan 608-737, Korea. *E-mail: ykim@pknu.ac.kr*

Received December 8, 2006

Three different phosphonated trisbipyridine ruthenium complexes, $[(4\text{-}CH_3\text{-}4'\text{-}CH_2PO(OH)_2\text{-}2,2'\text{-bipyridine})(bpy)_2Ru]\cdot(PF_6)_2$ (Ru-P1), $[(4\text{-}CH_3\text{-}4'\text{-}CH_2PO(OH)_2\text{-}2,2'\text{-bipyridine})_3Ru]\cdot(PF_6)_2$ (Ru-P2), and $[(4,4'\text{-}CH_2PO(OH)_2\text{-}2,2'\text{-bipyridine})_3Ru]\cdot(PF_6)_2$ (Ru-P3) were synthesized and their photochemical and electrochemical properties were studied. These ruthenium complexes were strongly adsorbed on the surface of the layered metal oxide semiconductor $K_4Nb_6O_{17}$ that was partially acid-exchanged and sensitized up to pH 10, while the carboxylated ruthenium complex, $(4,4'\text{-}COOH\text{-}2,2'\text{-bipyridine})_3Ru\cdot Cl_2$ (Ru-C) that was previously studied was sensitized only below pH 4. The visible light water reduction at $K_4Nb_6O_{17}$ that was internally platinized and sensitized by these phosphonated Ru-complexes was comparatively studied using a reversible electron donor iodide.

Key Words : Layered metal oxide semiconductor, $K_4Nb_6O_{17}$, Phosphonated trisbipyridine ruthenium complexes, Water splitting

Introduction

Water splitting into molecular hydrogen and oxygen by solar light is one of most important projects for energy solution in the next generation.[1] In the field of photocatalysis there has been reported that the stoichiometric water splitting into molecular hydrogen and oxygen could be achieved by the band-gap excitation of some metal oxide semiconductors that have structural characteristics and specific catalytic sites.[2] However, those water cleavages in the most of cases utilized ultra violet light that is a very small portion of the entire solar spectrum. Therefore, in order to increase solar energy conversion efficiency the photocatalysts have been doped with some other metal ions to respond to visible light that occupies major portion of solar spectrum.[3]

Another strategy to utilize visible light in solar spectrum is the sensitization of metal oxide semiconductor by visible light absorbing molecules that has been now well-known in the field of solar cell as the dye-sensitized solar cell, namely Grätzel's cell[4] since the introduction by Gerisher in 1972.[5] Although the strategy was so successful in the field of photoelectrochemical cell, there is little example of photocatalyst reported yet, which shows water splitting into hydrogen and oxygen by this dye-sensitization. However, one of us reported that tris(2,2'-bipyridyl-4,4'-dicarboxylate)ruthenium-sensitized $K_4Nb_6O_{17}$ particles[6] and Nb_2O_5-zeolite composites[7] could generate hydrogen from a *nonsacrificial* electron donor by visible light. These systems showed the possibility for the visible light water cleavage by the dye-sensitized semiconductor system by preventing energy-dissipating recombination reaction through the compartmentalization of oxidation and reduction sites in nano-scale level. The schematic energy diagram for these systems is shown in Scheme 1.

Although the visible light absorbing sensitizer, tris(2,2'-bipyridyl-4,4'-dicarboxylate) ruthenium complex, which was used in the nonsacrificial water reduction photocatalysts, was somehow successful to attach on the surface of metal oxide semiconductors and transfer electrons efficiently by visible light excitation, the attachment and electron transfer on the semiconductors were limited only in low solution pH (< pH 4).[8] To get the optimized condition for water cleavage, the tuning of pH condition is essential for these sensitized semiconductor systems. Recent studies[9] demonstrated that some phosphonated ruthenium complexes could be also strongly adsorbed on the surface of a metal oxide semiconductor, especially TiO_2 and the efficient electron transfer

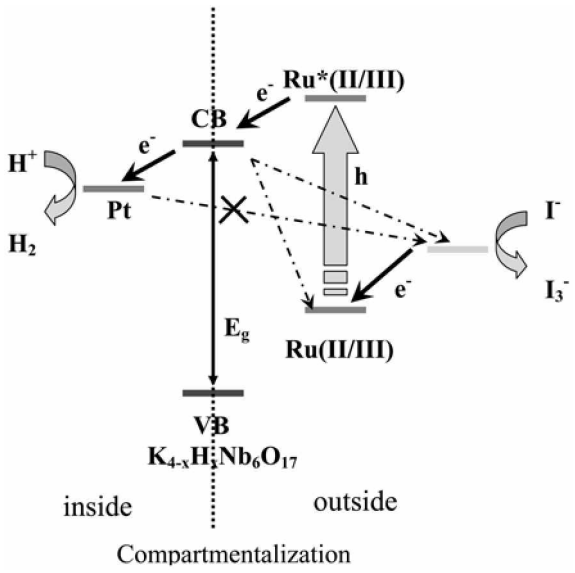

Scheme 1. Schematic drawing of energy diagram in the dye-sensitized photocatalytic system. The broken line arrows indicate the possible charge recombination paths.

quenching could be occurred. And this adsorption was known to be less sensitive to solution pH in the range of pH 2-10 than in the case of the carboxylated complexes. Therefore, we have applied several (phosphonic acid)-functionalized ruthenium complexes to nonsacrificial $K_4Nb_{16}O_{17}$ semiconductor system instead of the previously used carboxylated ruthenium complex and studied the hydrogen evolution efficiency comparatively in this study.

Experimental

Materials. 4,4'-dimethyl-2,2'-dipyridyl (99%), 2,2'-bipyridine-4,4'-dicarboxylic acid (98%), $RuCl_3 \cdot xH_2O$ (99.98 %), NH_4PF_6 (99.99%) Nb_2O_5 (99.99%), $Pt(NH_3)_4Cl_2 \cdot xH_2O$ (99.99%), and triethylphosphite (98%) were purchased from Aldrich and used as obtained. $Ru(bpy)_2Cl_2 \cdot xH_2O$, was prepared by a literature method.[10] All other chemicals were reagent grade and water was purified in Barnstead Nanopure II water purification system to 18.0 MW·cm resistivity. The preparation of $K_4Nb_6O_{17}$ and its platinization were performed as previously described.[6] $K_4Nb_6O_{17}$ was prepared by heating the stoichiometric mixture of Nb_2O_5 and K_2CO_3 at 1050 °C for 2 days. The platinization of $K_4Nb_6O_{17}$ was done by ion-exchange with $Pt(NH_3)_4Cl_2$ for 3 days in an aqueous solution and thermal reduction by H_2 at 450 °C. The loading amount of platinum was fixed as 0.05 wt% before aqua regia treatment in all experiments. The platinized $K_4Nb_6O_{17}$ was treated with aqua regia at about 90 °C for an hour to remove platinum exposed on surface. The subsequent acid exchange was performed in 0.1 M HCl for 2 days. This internally platinized and acid-exchanged hexaniobate is denoted as $K_{4-x}H_xNb_6O_{17}$/Pt. The ruthenium complexes were adsorbed onto $K_{4-x}H_xNb_6O_{17}$/Pt by adding appropriate amounts from their aqueous solutions to an aqueous suspension of $K_{4-x}H_xNb_6O_{17}$/Pt. Typically 5×10^{-7} mol/g loading level was used for all hydrogen evolution experiments.

Apparatus. UV-Vis absorption and emission spectra were measured with Varian Cary 1 spectrophotometer and Jasco FR6300 spectrofluorometer, respectively. X-ray diffraction patterns were recorded by Rigaku D/Max-2400 with Cu$K\alpha$ source line and 0.01 °/s scan rate. Scanning electron micrographs were taken by Hitachi U-420 with acceleration voltage 20 kV. Cyclic voltammograms were measured by EG&G PAR 263A potentiostat in a standard three electrode cell with glassy carbon working electrode, SCE reference electrode and aqueous 0.1 M KCl or $NaClO_4$ electrolyte solution. The steady-state photolyses were performed in a silicon rubber-septumed quartz reaction vessel with flat window. The total volume of the vessel was 48 mL and the volume of the photocatalyst suspension was 29 mL. 300 W Xe(Hg) arc lamp (ILC PS200-1) was served as light source equipped with Pyrex water filter and 410 nm cut-off or 450 nm (± 10 nm) interference filter. The light intensities measured by Molectron P10 power meter were 162 mW/cm^2 and 55 mW/cm^2 with the cut-off (> 410 nm) and the interference (450 ± 10 nm) filters, respectively. The sample suspension and headspace in the vessel were thoroughly purged by Ar gas for 30 min before irradiation. The evolved hydrogen was collected in the headspace and analyzed by gas chromatography with molecular sieve (5A) column and thermal conductivity detector (Shimadzu 14-A).

Synthesis of [(2,2'-bipyridine-4,4'-dicarboxylic acid)$_3$-Ru]·Cl$_2$ (Ru-C). The synthesis was basically followed by a literature method.[11] The mixture of 2,2'-bipyridine-4,4'-dicarboxylic acid and $RuCl_3 \cdot xH_2O$ in 3.2:1 molar ratio was refluxed in dimethyl formamide (DMF) under N_2 for a week. After evaporating the solvent, the reaction mixture was separated by silica gel column chromatography with the elution solution (CH_3CN:H_2O:sat'd KNO_3 = 5:4:1). The separated product was dissolved in H_2O and precipitated by adding conc. HCl (yield: 30%).

[(4-CH$_3$-4'-CH$_2$PO(OH)$_2$-2,2'-bipyridine)(bpy)$_2$Ru]·(PF$_6$)$_2$ (Ru-P1). 4-CH_3-4'-CH_2Br-2,2'-bipyridine was first prepared by photoreaction of 4,4'-dimethyl-2,2'-bipyridine and Br_2 (1:1 molar ratio) in two phase solvents of H_2O and CCl_4. 40 mL of water was added to 1.0 g of 4,4'-dimethyl-2,2'-dipyridyl in 60 mL of CCl_4 and degassed with nitrogen gas for an hour. 0.14 mL of Br_2 was added to the mixture and visible light (> 450 nm) was irradiated to the reaction mixture for about 2 hours under N_2. After adding 100 mL of 0.1 M Na_2CO_3 to neutralize the evolved HBr, CCl_4 layer where the product was mostly dissolved was separated from the aqueous layer and the product was isolated by evaporating the solvent. The final product was separated by silica gel column chromatography with the eluent of CH_2Cl_2/acetone (99.8:0.2 v/v) and recrystalized with diethyl ether (yield: 23%). 4-CH_3-4'-CH_2Br-2,2'-bipyridine was converted to 4-CH_3-4'-CH_2PO-(OCH_2CH_3)$_2$-2,2'-bipyridine by the reaction with triethyl phosphite according to a method of Hupp *et al.*'s.[9(a)] The mixture of $Ru(bpy)_2Cl_2 \cdot xH_2O$ and 4-CH_3-4'-CH_2PO(OCH_2-CH_3)$_2$-2,2'-bipyridine in 1:1.2 molar ratio was refluxed in DMF at 155 °C for 24 hours. After removing the solvent the unreacted ligands were extracted with chloroform and the product was refluxed in 6 M HCl solution for a day to hydrolyze the phosphonate group to phosphonic acid. The final product was purified by silica gel column chromatography with the elution solution (CH_3CN:H_2O:sat'd KNO_3 = 5:4:1). After removing KNO_3 by adding acetone, the product was isolated by adding NH_4PF_6 (yield: 25%).

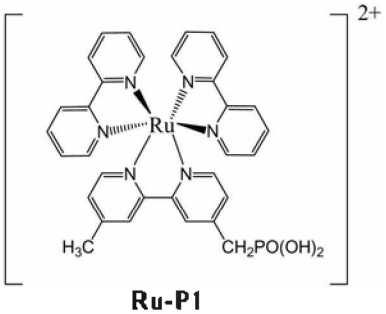

Ru-P1

[(4-CH$_3$-4'-CH$_2$PO(OH)$_2$-2,2'-bipyridine)$_3$Ru]·(PF$_6$)$_2$ (Ru-P2). The mixture of $RuCl_3 \cdot xH_2O$ and 4-CH_3-4'-CH_2PO(OCH_2CH_3)$_2$-2,2'-bipyridine in 1:3.2 molar ratio was

refluxed in DMF solvent at 155 °C for 24 hours. After extracting the unreacted ligand with chloroform the product was hydrolyzed in 6 M HCl solution and isolated as PF_6 salt in the same way as Ru-P1 (yield: 30%).

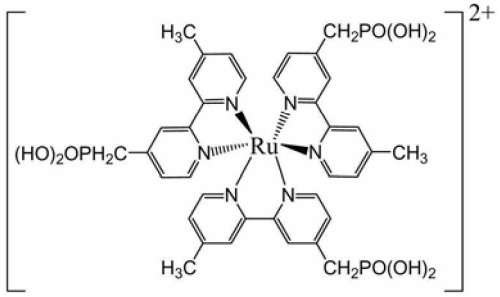

Ru-P2

[(4,4'-$CH_2PO(OH)_2$-2,2'-bipyridine)$_3$Ru]·(PF_6)$_2$ (Ru-P3). The synthesis of this complex was previously described.[9(a)] 4,4'-bis(Bromomethyl)-2,2'-bipyridine was first prepared by the radical reaction of 4,4'-dimethyl-2,2'-bipyridine and *N*-bromosuccinimide with azobis(isobutyronitrile) as an initiator in CCl_4 solvent at 80 °C under Ar.[12] 4,4'-bis(Bromomethyl)-2,2'-bipyridine was refluxed in triehtyl phosphite for 6 hours to give 4,4'-bis($CH_2PO(OCH_2CH_3)_2$)-2,2'-bipyridine (yield: 25%). The mixture of $RuCl_3 \cdot xH_2O$ and 4,4'-bis($CH_2PO(OCH_2CH_3)_2$)-2,2'-bipyridine in 1:3.2 molar ratio was refluxed in methoxyethanol with $NH_2OH \cdot HCl$ under N_2 at 130 °C for a week. The unreacted ligand was extracted with $CHCl_3$. The product was refluxed in 6 M HCl at 122 °C for one day to hydrolyze phosphonate to phosphonic acid. After removing H_2O and HCl the final product was dissolved in H_2O and precipitated by adding NH_4PF_6 (yield: 80%).

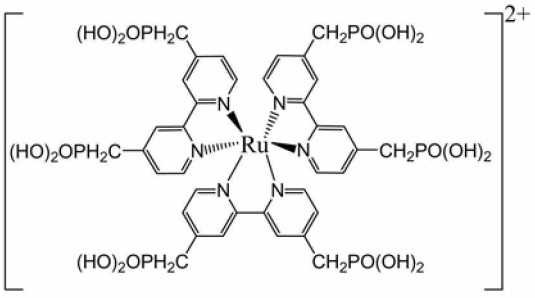

Ru-P3

Results and Discussion

Photochemical and electrochemical properties of the phosphonated ruthenium complexes. Figure 1 shows the absorption spectra of the phosphonated ruthenium complexes as dissolved in H_2O. The pH dependence of the absorption spectra was negligible in the range of pH 4 to 10. As the number of phosphonic acid increased, the absorption maximum slightly shifted to red. It shifted to red in all three cases compared to that of non-functionalized $Ru(bpy)_3^{2+}$ (454 nm) whereas they are in shorter wavelength than that of Ru-C that was the previously used carboxylated ruthenium

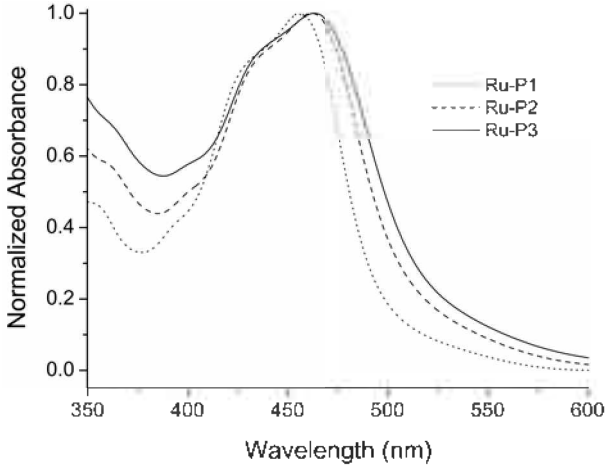

Figure 1. The normalized UV-Vis absorption spectra of the phosphonated trisbipyridine ruthenium complexes in aqueous solutions (*ca.* 2×10^{-5} M).

complex (466 nm). The electron withdrawing nature of phosphonic acid might slightly stabilize the π^* orbital of the bipyridine ligand and lower the energy level of MLCT excited state.[9(f)] But the energy shift may not be significant because of electron-donating methyl group between phosphonic acid and bipyridine. In Figure 2 the emission spectra of three phosphonated ruthenium complexes are shown at three different pHs. As pH increased, the emission maxima of all three complexes shifted to longer wavelength (5-10 nm) until pH 7. The shift of the maximum was not pronounced above pH 7. Since the previously studied phosphonated ruthenium complexes showed the values of about 2 and 7 for pK_1 and pK_2, respectively,[13,14] the most deprotonated form will be predominant above pH 7. Therefore the emission spectra will not be much influenced by pH above 7. In the range of pH 2-7 the single protonated form will be predominant but the ratio of the protonated to the deprotonated form will be changed by pH values. This means that the excited states of the complexes were affected by proton dissociation equilibria. The carboxylated ruthenium complex, Ru-C also showed pH dependence of the emission spectrum but the tendency was opposite of that of our Ru-Ps: As the pH increased, emission maximum shifted to shorter wavelength.[15] This phenomenon was explained by the acid dissociation difference between the ground state and excited state complexes. Montalti *et al.*[14] also reported that the pH dependence of emission spectra of a phosphonic acid-functionalized ruthenium complex showed the similar tendency with the carboxylated complex. This different pH dependence might result from the major structural difference between them. While the phosphonic acid in our complexes is connected to bipyridine ligand through a spacer electron-donating methyl group, the phosphonic acid in Montalti's complex and carboxylic acid in Ru-C were attached directly to the bipyridine without any spacer.

Figure 3 shows the cyclic voltammograms of all three complexes in aqueous KCl solution. All complexes exhibited quasi-reversible redox peaks assigned to Ru(II/III). The

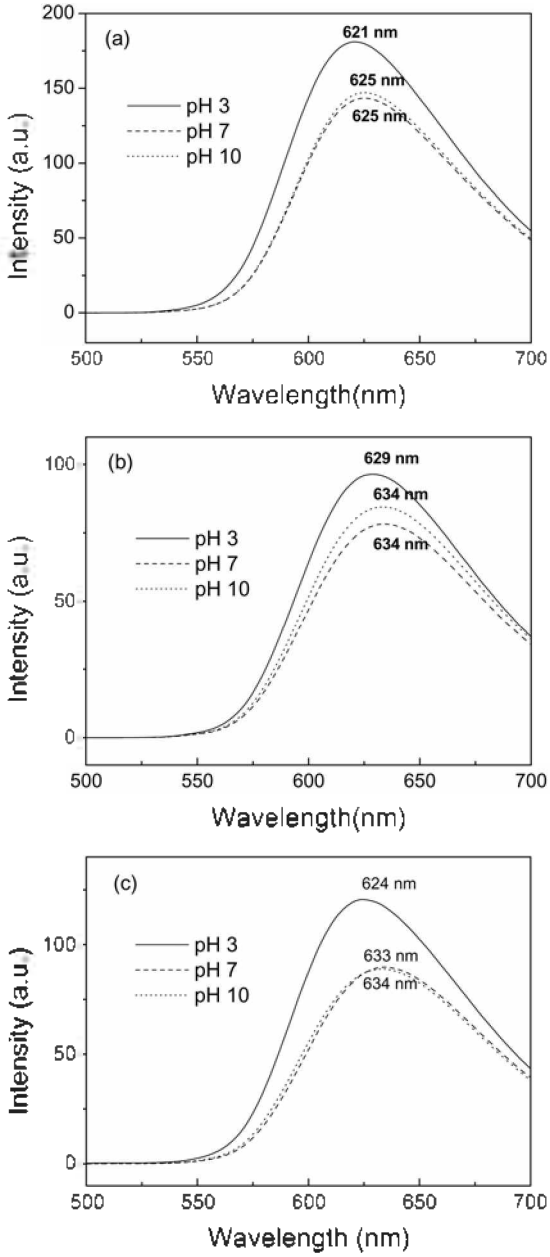

Figrue 2. Emission spectra of the ruthenium complexes of (a) Ru-P1, (b) Ru-P2 and (c) Ru-P3 in aqueous solutions of several pHs (*ca.* 1.0×10^{-5} M, excited at 455 nm).

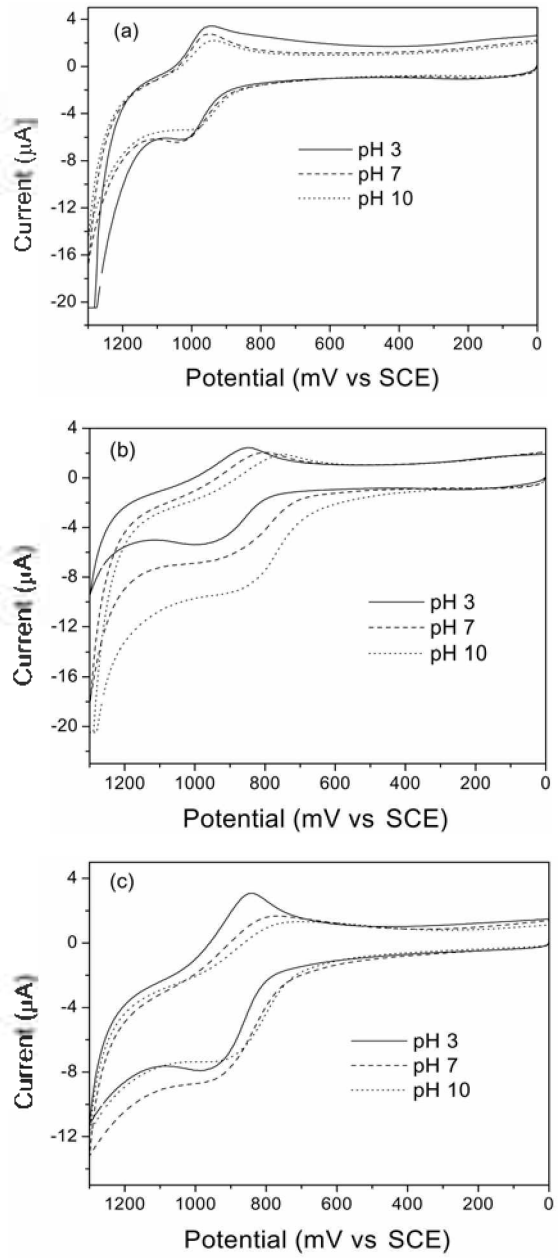

Figure 3. Cyclic voltammograms of the ruthenium complexes of (a) Ru-P1, (b) Ru-P2 and (c) Ru-P3 at several pHs (2×10^{-5} M, scan rate: 50 mV/s, 0.1 M $NaOCl_4$).

half-wave potential ($E_{1/2}$) decreased as the number of phosphonic acid increased and as the solution pH increased in the same compound. The potentials were shifted negatively to 50-200 mV and 150-210 mV compared with those of unsubstituted ruthenium trisbipyridine complex (+1.049 V s SCE at pH 7) and Ru-C (+1.144 V *vs* SCE at pH 7), respectively in the same condition. The oxidation potentials of Ru(II/III) in these complexes seemed to be more influenced by the electron donating spacer methyl group rather than electron withdrawing terminal phosphonic acid because the electron withdrawing group in the ligand shifted the potential positively. However, the pH dependence of $E_{1/2}$ implies that the redox process involves slight proton-coupling in phosphonic acid group although the process does not follow the Nernst relation (59 mV/pH).

The excited state redox potential of the complex, $E_{1/2}$ ($Ru^{*2+/3+}$) can be roughly estimated by adding the maximum emission energy to the ground state potential, $E_{1/2}(Ru^{2+/3+})$. The potentials also shifted to negative values as the solution pH increased except Ru-P1 whose pH dependence is negligible. And all potentials are higher than that of the carboxylated complex, Ru-C. This means that the phosphonated complexes can do transfer electrons better to the conduction band of metal oxide semiconductor than the carboxylated complex does because of higher driving forces. Table 1 summarizes the spectroscopic and redox properties of the

Table 1. The emission maxima and the redox potentials of the ruthenium complexes in ground-state and excited-state at various pHs

Complexes	pH	Absorption λ_{max} (nm)	$E_{1/2}$ ($Ru^{3+/*2+}$) (V *vs.* SCE)	Emission λ_{max} (nm)	$E_{1/2}$($Ru^{3+/*2+}$) (V *vs.* SCE)
Ru-P1	3	457	0.990	621	−1.007
	7		0.994	625	−0.990
	10		0.975	625	−1.009
Ru-P2	3	462	0.915	629	−1.056
	7		0.857	634	−1.099
	10		0.815	634	−1.141
Ru-P3	3	463	0.907	624	−1.080
	7		0.850	634	−1.106
	10		0.805	633	−1.154
Ru-C	7	466	1.144	628	−0.830

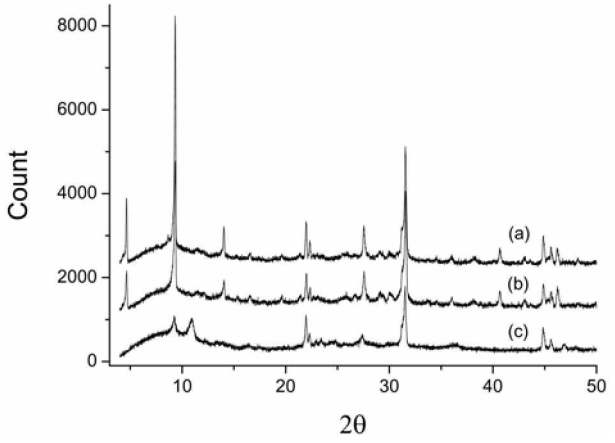

Figure 4. XRD diffraction patterns of (a) $K_4Nb_6O_{17}$, (b) platinized $K_4Nb_6O_{17}$ and (c) $K_{4-x}H_xNb_6O_{17}$/Pt.

complexes at different pH values.

Characterization of the platinized $K_4Nb_{16}O_{17}$. Figure 4 shows XRD patterns of $K_4Nb_6O_{17}$, platinized $K_4Nb_6O_{17}$ ($K_4Nb_6O_{17}$/Pt) and platinized $K_4Nb_6O_{17}$ after the treatment of aqua regia ($K_{4-x}H_xNb_6O_{17}$/Pt). The XRD pattern of the untreated sample indicates a typical hydrated $K_4Nb_6O_{17}$ ($K_4Nb_6O_{17}\cdot 3H_2O$) that has orthorhombic unit cell. The estimated unit cell parameters were 8.13, 37.33 and 6.40 Å for a, b and c, respectively. The values are very close to the reported values (a = 7.85, b = 37.9, c = 6.46 Å)[16] except the parameter a. The slightly larger value of a might be due to the elongated structure in the direction of a axis. But the parameter b that determines the interlayer spacing confirmed the degree of hydrations ($3H_2O$). The pattern of the platinized sample is not different from that of the untreated one. $K_4Nb_6O_{17}\cdot 3H_2O$ is a typical layered material that has two distinct interlayers where one is hydrated (interlayer I) and the other is unhydrated (interlayer II). The interlayer I can be ion-changed with divalent cations whereas the interlayer II can be ion-exchanged with only monovalent cation.[17] Although most of Pt was deposited into the interlayer I of the hexaniobate by cation exchange, there is no appreciable

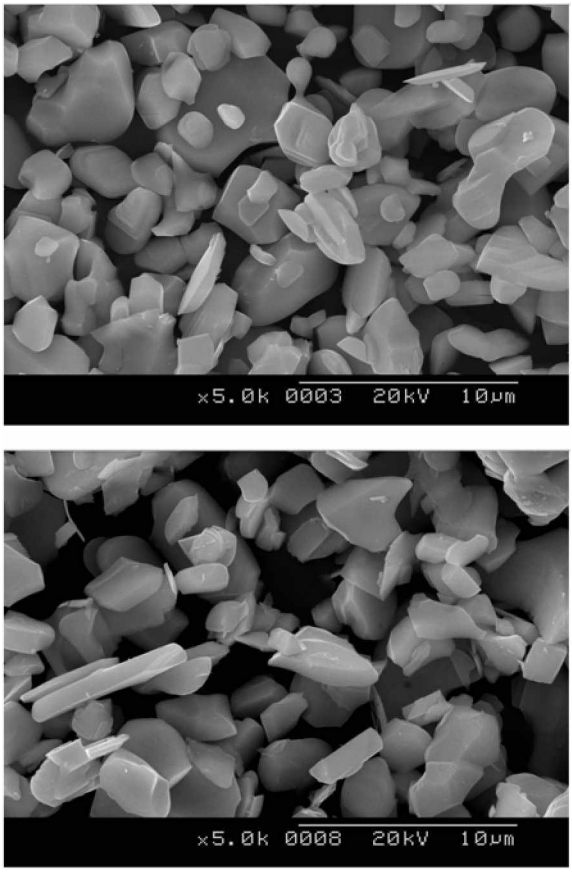

Figrue 5. Scanning electron microscopic pictures of $K_4Nb_6O_{17}$ (top) and $K_{4-x}H_xNb_6O_{17}$/Pt (bottom).

change in structure due to the intercalation because the amount of deposited Pt was so small (0.05 wt%). In order to remove platinum that resides on the outer surface of the hexaniobate, the platinized hexaniobate was treated with hot aqua regia as previously studied.[6] The platinized and aqua regia-treated sample shows the different XRD pattern from those of the unplatinized and the platinized but untreated ones. Because K^+ ions in interlayers were partially exchanged with proton in high acidic condition of aqua regia, the strongest (040) diffraction layer that was due to interlayer spacing was changed to two peaks that correspond to narrower interlayer spacing than the original one.

The scanning electron microscopic pictures of untreated $K_4Nb_6O_{17}$ and $K_{4-x}H_xNb_6O_{17}$/Pt are shown in Figure 5. As shown is the figure, the particles are of disk type that is typical in layered materials and their sizes are in the range of 1-5 μm. The average particle size is about 3-4 μm in diameter. The comparison between untreated $K_4Nb_6O_{17}$ and $K_{4-x}H_xNb_6O_{17}$/Pt in the pictures confirms that there was no morphological change or damage when the sample was treated with hot aqua regia.

Photochemical hydrogen evolutions of the sensitized Pt/$K_{4-x}H_xNb_6O_{17}$ from KI solution. The phosphonated ruthenium complexes (Ru-Ps) were all strongly adsorbed on the surface of $K_{4-x}H_xNb_6O_{17}$/Pt up to 2-3 $\times$ 10^{-6} mol/g when they were added to an aqueous suspension of

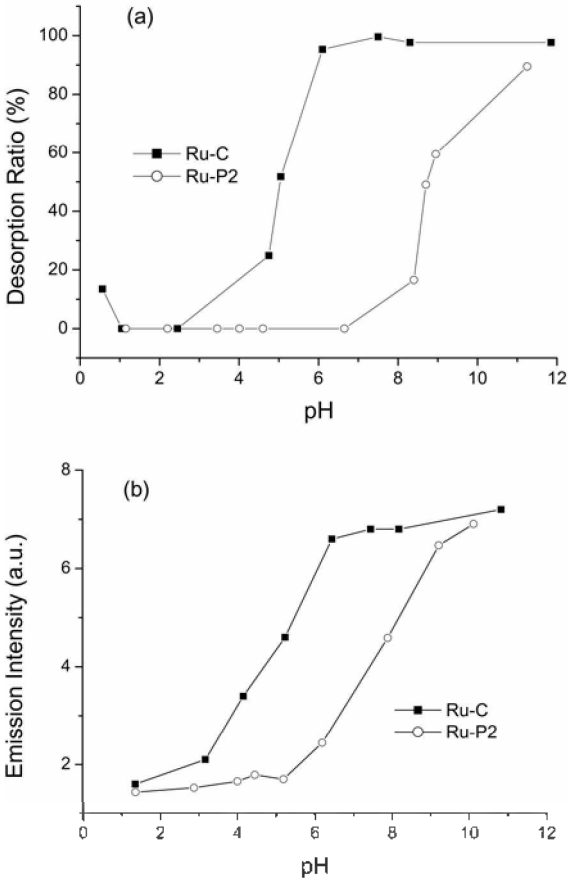

Figure 6. pH dependences of the desorption ratio (a) and the emission intensity (b) of Ru-P2 (1.0×10^{-6} mol/g) on Pt/$K_{4-X}H_XNb_6O_{17}$ in aqueous suspension.

$K_{4-X}H_XNb_6O_{17}$/Pt. Figure 6 shows pH dependence of the desorption ratio and emission intensity of Ru-P2 and Ru-C on $K_{4-X}H_XNb_6O_{17}$/Pt. The desorption ratio was determined by absorbance measurement of the desorbed complexes. Ru-P2 remained on the platinized hexaniobate until pH 8 and about 20% of the complex was still on the surface even at pH 10, whilst Ru-C started to be desorbed at pH 4 and was completely desorbed at pH 7. The results for Ru-P1 and Ru-P3 were also very similar with that of Ru-P2 and not shown here. This result is consistent with that of Ru-P3 on TiO_2 that was previously reported.[5(a)] The emission intensities of Ru-Ps on $K_{4-X}H_XNb_6O_{17}$/Pt showed also the same pH dependence: the emission from Ru-P2 was almost completely quenched at the lower pH than 6 and the emission intensity started to increase at pH 6 and was saturated at about pH 10 as shown in Figure 6(b). This result tells that all Ru-Ps are attached on the surface of $K_{4-X}H_XNb_6O_{17}$/Pt and the excited state quenching occurs below pH 7 whereas this is possible only below pH 4 in the case of Ru-C. The comparison of pH dependence of the desorption ratio and emission intensity tells that the emission intensity starts to increase above pH 7 although the complex still remained on the surface of the hexaniobate. This might be due to the elevated conduction band edge potential at high pH. The driving force of electron transfer from the excited ruthenium complex to the conduction band decreases and the quenching rate might decrease. We would like to point out that the elevated conduction band potential at high pH is not only due to the Helmholtz potential by the surface-adsorbed ions but also due to the change of interlayer composition as discussed in the previous report.[5(b)]

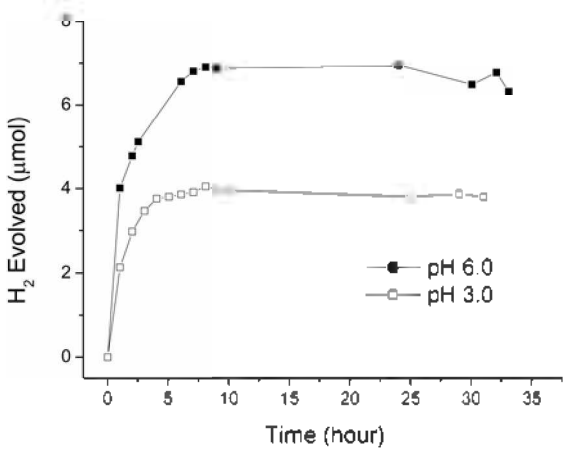

Figure 7. Hydrogen evolutions from Pt/$K_{4-X}H_XNb_6O_{17}$/Ru-P1 in 0.1 M KI solution at several pHs ($h\nu > 410$ nm).

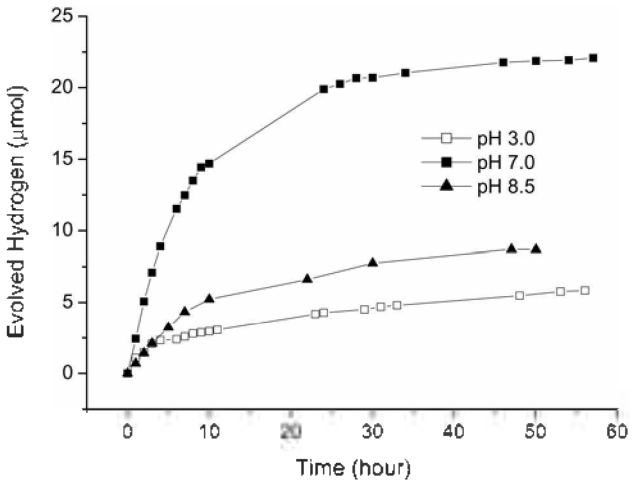

Figure 8. Hydrogen evolutions from Pt/$K_{4-X}H_XNb_6O_{17}$/Ru-P2 in 0.1 M KI solution at several pHs ($h\nu > 410$ nm).

Figure 7 and 8 show the hydrogen evolutions from $K_{4-X}H_XNb_6O_{17}$/Pt sensitized by Ru-P1 and Ru-2, respectively in 0.1 M KI solution under the illumination of visible light (> 410 nm). As shown in the figures the amounts of evolved hydrogen were much higher at pH 6-7 than at pH 3 in both cases. Whilst the hydrogen evolution for Ru-C was possible only below pH 4, the phosphonated complexes enabled the hydrogen evolution at higher pH than 4 and showed better efficiency at higher pH. The hydrogen evolution efficiency in this system depends upon several factors. As shown in Scheme 1, the excited complex was first quenched and oxidized by the electron transfer to conduction band of the hexaniobate and the injected electrons in the conduction band were transferred to the internal platinum site to reduce H_2O or H^+ to H_2. To regenerate the ruthenium complex,

iodide in solution phase donates electron to the complex and is oxidized to I_3^- finally. If this cycle is not interrupted by other factors, the hydrogen evolution will continue until the donor iodides in solution are depleted although the evolution rate will decrease with time. However, there are several charge recombination processes that interrupt the cycle. There are three major recombination processes possible in this system as indicated in Scheme 1: the recombinations between the injected conduction band electron and the oxidized ruthenium complex, between the conduction band electron and the oxidized iodide in solution, and between the evolved hydrogen and the oxidized iodide. The first recombination was known to be as much as 10^5 times slower than the forward quenching rate and this fact makes the dye-sensitized semiconductor system very useful for solar energy conversion. The third recombination was intentionally blocked by the internal platinization and inaccessibility of the oxidized iodide to the hydrogen evolution site as mentioned in Introduction. Therefore the hydrogen evolution efficiency in this system is thought to depend mostly on the second recombination that occurs between the conduction band electron and the oxidized iodide. Saupe *et al.* studied this recombination kinetics in the same sensitized hexaniobate system with a different ruthenium complex.[18] They have shown that the recombination rate can be retarded when the sensitized hexaniobate was surface-modified with anionic blocking layers such as exfoliated $[TiNbO_5]_n^{n-}$ and poly(styrenesulfonate) and the initial hydrogen evolution efficiency increased by factors of 3-5.

The pH dependence of the hydrogen evolution in these phosphonated ruthenium complexes sensitized systems can be due to the several pH dependent factors such as the conduction band potential, the excited state redox potentials of the complexes, the electron transfer kinetics between the oxidized complexes and donor iodide, and the recombination kinetics between the triodes and conduction band electrons. The pH dependence of conduction band potential comes from Helmholtz potential shift and interlayer composition change in the hexaniobate as mentioned above. The pH dependence of excited state redox potentials of the complexes are shown in Table 1. The pH dependence of the electron transfer kinetics between the oxidized complexes and donor iodide can be due to the charge interaction between iodide and the unattached phosphonate group in the complexes. In this case the kinetics can be retarded at higher pH because the deprotonated phosphonate is negatively charged at high pH and repel the negative iodide. The charge recombination rate between the oxidized iodide and the injected conduction band electron can be also retarded at high pH because the surface of the hexaniobate at high pH will be negatively charged and it also repels the negatively charged triiodide.

The higher hydrogen efficiency at higher pH shown in Figure 7 and 8 can be mainly due to the higher conduction band potential that is originated from the interlayer composition change not from Helmholtz potential shift and the retarded charge recombination between the oxidized donor and conduction band electrons. Since the composition of K^+ in $K_{4-x}H_xNb_6O_{17}$ changes from x = 0 in as-prepared to x = 2 in fully acid-exchanged form and the pH of the suspension changed from about 10 to 3 for $K_4Nb_6O_{17}$ and $K_{4-x}H_xNb_6O_{17}$, respectively.[6(b)] the interlayer composition of K^+ in the compound must change as the suspension pH changes. The conduction band shift due to the Helmholtz layer potential change that follows Nernst relation is not beneficial because proton reduction potential also shifts exactly following the Nernst relation. However, the increase of alkali metal ions in interlayer composition at higher pH will increase conduction band potential due to the electronegativity change in the semiconductor as discussed in the previous paper.[6(b)] As shown in the study of Saupe *et al.*'s[19] the charge recombination between the oxidized iodide and conduction band electron can dramatically effect the hydrogen evolution efficiency. Therefore better hydrogen efficiency at high pH in this system must be partly attributed from the retarded charge recombination. The surface anchoring by phosphonic acid group enables this only by the pH effect without a special surface modification as shown in Saupe *et al.*'s study.

The hydrogen evolution from Ru-P1 complex shown in Figure 7 ceased after about 5 hours. This apparent stop is due to the charge recombination between oxidized I_3^- and injected conduction electrons rather than due to the deactivation of the photocatalyst because the hydrogen evolution rate was restored when the solution was refreshed with new KI solution as shown in a previous study.[6(a)] As the concentration of I_3^- increases the recombination rate between conduction band electrons and I_3^- increases and compete with hydrogen evolution. This stop occurred more quickly with Ru-P1 than with Ru-C in the previous studies.[6] Whereas there is no negative charge exposed to solution for Ru-P1, Ru-C has six carboxyl groups and there are four carboxyl groups in solution that are partially deprotonated and negatively charged. These negative charges repel the oxidized iodide since the oxidized iodide has also negatively

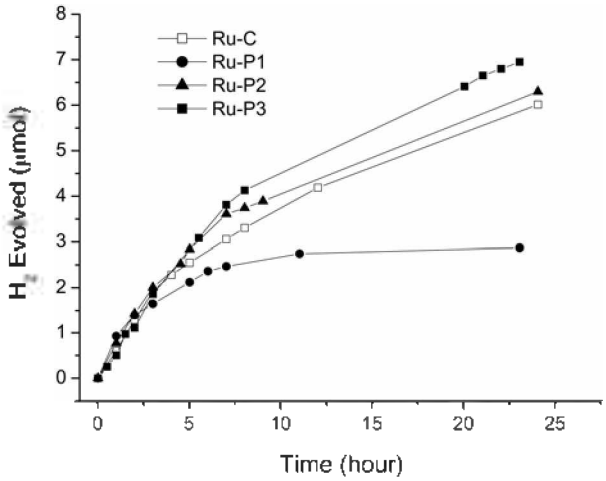

Figrue 9. Hydrogen evolutions from Pt/$K_{4-x}H_xNb_6O_{17}$/Ru-complexes in 0.1 M KI solution ($h\nu$ = 450 ± 10 nm). pH of the solutions were 4 and 7 for the carboxylated and phosphonated complexes, respectively.

charged as triiodide and contribute to the slow down of the recombination. Therefore, we might expect that slower stopping for Ru-P2 and Ru-P3 than Ru-P1 where more negatively charged phosphonate groups are available in solution side. Indeed, Ru-P2 and Ru-P3 showed the same trend as Ru-C as shown in Figure 8 and 9. In Figure 9 the hydrogen evolutions were compared for four different sensitizers in the same condition except optimized pH. The quantum efficiencies for the initial hydrogen evolution rate were estimated to be 0.55, 0.46, 0.30 and 0.36% for Ru-P1, Ru-P2, Ru-P3 and Ru-C, respectively. The highest efficiency for Ru-P1 can not be explained by the energetics because the driving force of electron-transfer quenching for Ru-P1 is the smallest among the three complexes as shown in Table 1. It may be explained by better electron donor accessibility to the oxidized complex. Since Ru-P1 does not have negative ion exposed outer, negative iodide can more readily approach to the oxidized complex and result in the higher electron transfer efficiency, while the outer phosphonate groups in Ru-P2 and Ru-P3 might hinder the approach of iodide. However, the long term efficiency seems to be governed by charge recombination between the oxidized iodide and the injected conduction band electron. The negatively charged phosphonate group repelled the oxidized iodide from the surface of the niobate and the recombination was partially blocked.

Conclusions

Three different types of the phosphonated trisbipyridine ruthenium complexes were utilized for photochemical hydrogen evolution in the internally platinized layered metal oxide semiconductor, $K_{4-x}H_xNb_6O_{17}$ from nonsacrificial iodide solution. The phosphonic acid group for surface-anchoring in the complexes, instead of carboxylic acid previously studied, enables us to study the pH dependence on hydrogen evolution for this complex system. In all three cases maximum hydrogen evolution was obtained at neutral pH condition rather than acidic or basic. The quantum efficiencies for the initial hydrogen evolution rate were estimated to be 0.55, 0.46, 0.30 for Ru-P1, Ru-P2 and Ru-P3, respectively. These values are somehow higher or similar with that of the carboxylated ruthenium complex (Ru-C) that was previously studied. The hydrogen evolution rate in this dye-sensitized semiconductor photocatalyst was governed by the accessibilities of electron donor and oxidized donor to the sensitizers and the surface of semiconductor, respectively, which is controlled by the solution pH rather than the energetics of the photoinduced electron transfer.

Acknowledgement. This work was supported by Pukyong National University Research Foundation Grant in 2004.

References

1. (a) Dunn, S. *Int. J. Hydrogen Energy* **2002**, *27*, 235. (b) Bak, T.; Nowotny, J.; Rekas, M.; Sorrell, C. C. *Int. J. Hydrogen Energy* **2002**, *27*, 991.
2. (a) Domen, K.; Kudo, A.; Shinozaki, A.; Tanaka, A.; Maruya, K.; Onishi, T. *J. Chem. Soc. Chem. Comm.* **1986**, 356. (b) Sayama, K.; Tanaka, A.; Domen, K.; Maruya, K.; Onishi, T. *J. Phys. Chem.* **1991**, *95*, 1345. (c) Miseki, Y.; Kato, H.; Kudo, A. *Chem. Lett.* **2005**, *34*, 54.
3. (a) Yamasita, D.; Takata, T.; Hara, M.; Kondo, J. N.; Domen, K. *Sol. State Ion.* **2004**, *172*, 591. (b) Kudo, A.; Kato, H.; Tsuji, I. *Chem. Lett.* **2004**, *33*, 1534.
4. (a) O'Regan, B.; Grätzel, M. *Nature* **1991**, *353*, 737. (b) Grätzel, M. *Nature* **2001**, *414*, 338. (c) Shin, Y.-J.; Kim, K. S.; Park, N.-G.; Kang, S. R.; Cang, S. H. *Bull. Korean Chem. Soc.* **2005**, *26*, 1929. (d) Kim, K. M.; Park, N.-G.; Kang, M. G.; Ryu, K. S.; Chang, S. H. *Bull. Korean Chem. Soc.* **2006**, *27*, 322.
5. Gerischer, H. *Photochem. Photobiol.* **1972**, *16*, 243.
6. (a) Kim, Y. I.; Salim, S. M.; Huq, J.; Mallouk, T. E. *J. Am. Chem. Soc.* **1991**, *113*, 9561 (b) Kim, Y. I.; Atherton, S. J.; Brigham, E. S.; Mallouk, T. E. *J. Phys. Chem.* **1993**, *97*, 11802.
7. Kim, Y. I.; Keller, S. W.; Krueger, J. S.; Yonemoto, E. H.; Saupe, G. B.; Mallouk, T. E. *J. Phys. Chem. B* **1997**, *101*, 2491.
8. Desilvestro, J.; Grätzel, M.; Kavan, L.; Moser, J. *J. Am. Chem. Soc.* **1985**, *107*, 2988.
9. (a) Yan, S. G.; Hupp, J. T. *J. Phys. Chem.* **1996**, *100*, 6867. (b) Péchy, P.; Rotzinger, F. P.; Nazeerudin, M. K.; Kohle, O.; Zakeeruddin, S. M.; Humphry-Baker, R.; Grätzel, M. *J. Chem. Soc. Chem. Commun.* **1995**, 65. (c) Trammell, S. A.; Wimbish, J. C.; Odobel, F.; Gallagher, L. A.; Narula, P. M.; Meyer, T. J. *J. Am. Chem. Soc.* **1998**, *120*, 13248. (d) Zaban, A.; Ferrere, S.; Gregg, B. A. *J. Phys. Chem. B* **1998**, *102*, 452. (f) Gillaizeau-Gauthier, I.; Odobel, F.; Alebbi, M.; Argazzi, R.; Costa, E.; Bignozzi, C. A.; Qu, P.; Meyer, G. J. *Inorg. Chem.* **2001**, *40*, 6073.
10. Sprintschnik, G. H. W.; Kirsch, P. P.; Whitten, D. G. *J. Am. Chem. Soc.* **1977**, *99*, 4947.
11. Park, J. W.; Ahn, J.; Lee, C. *J. Photochem. Photobiol. A: Chem.* **1995**, *86*, 89.
12. Gould, S.; Strouse, G. S.; Meyer, T. J.; Sullivan, B. P. *Inorg. Chem.* **1991**, *30*, 2942.
13. Zabri, H.; Gillaizeau, I.; Bignozzi, C. A.; Caramori, S.; Charlot, M.-F.; Cano-Boquera, J.; Odobel, F. *Inorg. Chem.* **2003**, *42*, 6655.
14. Montalti, M.; Wadhwa, S.; Kim, W. Y.; Kipp, R. A.; Schmehl, R. H. *Inorg. Chem.* **2000**, *39*, 76.
15. Giordano, P. J.; Bock, C. R.; Wrighton, M. S.; Interrante, L. V.; Williams, R. F. X. *J. Am. Chem. Soc.* **1977**, *99*, 3187.
16. Nassau, K.; Shiever, J. W.; Bernstein, J. L. *J. Electrochem. Soc.* **1969**, *116*, 348.
17. Kinomura, N.; Kumada, N.; Muto, K. *J. Chem. Soc. Dalton Trans.* **1985**, 234.
18. Saupe, G. B.; Mallouk, T. E.; Kim, W.; Schmehl, R. H. *J. Phys. Chem. B* **1997**, *101*, 2508.